CHEMISTRY OF MATERIALS

ARTICLE

pubs.acs.org/cm

Preparation of Microporous Carbon Fibers through Carbonization of Al-Based Porous Coordination Polymer (Al-PCP) with Furfuryl Alcohol

Logudurai Radhakrishnan,[†] Julien Reboul,[‡] Shuhei Furukawa,[‡,§] Pavuluri Srinivasu,[†] Susumu Kitagawa,[‡,§] and Yusuke Yamauchi[†,∥,⊥,*]

[†]World Premier International (WPI) Research Center for Materials Nanoarchitectonics, National Institute for Materials Science, 1-1 Namiki, Tsukuba 305-0044, Japan.

[‡]ERATO Kitagawa Integrated Pores Project, Japan Science and Technology Agency (JST), Kyoto Research Park Bldg #3, Shimogyo, Kyoto 600-8815, Japan

[§]Institute for Integrated Cell-Material Sciences (iCeMS), Kyoto University, Yoshida, Sakyo, Kyoto 606-8501, Japan

[∥]Faculty of Science and Engineering, Waseda University, 3-4-1 Okubo, Shinjuku, Tokyo 169-8555, Japan

[⊥]Precursory Research for Embryonic Science and Technology (PRESTO), Japan Science and Technology Agency (JST), 4-1-8 Honcho, Kawaguchi, Saitama 332-0012, Japan.

Supporting Information

ABSTRACT: Here, we report preparation of microporous carbon fibers through carbonization of an Al-based porous coordination polymer (Al-PCP) with furfuryl alcohol (FA) at 1000 °C under an inert gas atmosphere. During the carbonization process, the Al species are aggregated to form γ-alumina nanoparticles. After the carbonization, the γ-alumina nanoparticles (from 2 to 10 nm) are distributed over the entire area. By chemical treatment with HF, the γ-alumina nanoparticles can be easily removed to obtain pure microporous carbon. Interestingly, the fibrous morphology of the original Al-PCP is successfully retained after the carbonization process. The effect of the loading amount of FA into the porous networks of Al-PCP on properties of the obtained microporous carbon is carefully examined. From the N_2 adsorption−desorption isotherms, an increase in the BET surface area upon increasing the loading amount of FA is observed. The maximum surface area and pore volume of the obtained microporous carbon reach 513 m^2/g and 0.844 cc/g, respectively.

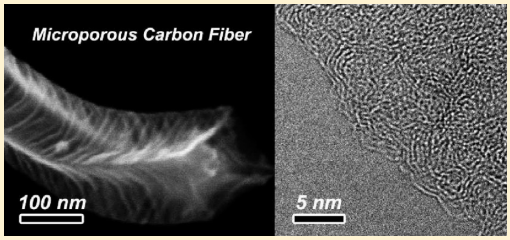

KEYWORDS: carbon materials, meso-porous materials, micro-porous materials, nanoimprinted materials, templated materials

1. INTRODUCTION

Porous carbon materials are one of the most studied materials because of their enormous applications in a huge variety of fields such as adsorbents, catalyst supports, and electrode materials. The effect of nature of templates, carbon sources or precursors, and carbonization conditions on the preparation of carbon materials has been investigated.[1,2] The preparation of carbon materials can be achieved through several synthetic methods, including chemical vapor deposition (CVD),[3] laser ablation,[4] electrical arc,[5] and so on.

Among these methods, nanocasting is an effective and successful way to prepare porous carbon materials.[6,7] For the preparation of carbon materials using the nanocasting method, porous inorganic templates such as zeolites, colloidal crystals, and ordered mesoporous silica materials are used with various carbon sources/precursors such as sucrose, furfuryl alcohol, phenol resins, polystyrene, mesophase pitches, and so on. Although the carbon materials have been known for decades, it was Ryoo et al. who first reported the preparation of mesoporous carbon materials using MCM-48 silica as a template.[8] This report uncluttered the gateway for the preparation of ordered mesoporous carbon materials with tunable pore size, structure, and chemical properties. Several mesoporous silica templates, such as MCM-48 (bicontinuous cubic *Ia*-3*d*), SBA-15 (2-D hexagonal *p6mm*), SBA-1 (cubic *Pm*-3*n*), and SBA-16 (cubic *Im*-3*m*), were also used in order to obtain their respective carbon replicas, CMK-4,[9] CMK-3,[10−14] CMK-2[15], and CMK-6[16], using various carbon sources/precursors. Kyotani and other researchers reported several works on the preparation of microporous carbon materials with high surface area using zeolites as templates.[17−21]

In the past decade, there has been rapid development on and much attention paid to porous coordination polymers (PCPs) or metal−organic frameworks (MOFs) because of their enormous applications, especially in the fields of gas separation and storage

Received: October 10, 2010
Revised: December 29, 2010
Published: January 27, 2011

and heterogeneous catalysis.[22−36] Porous coordination polymers (PCPs) are exciting and a fascinating genre of inorganic−organic hybrid materials, with unique properties like very high surface area and large pore volume, starkly surpassing far beyond zeolites and mesoporous materials. The PCPs containing metal ions and bridging organic ligands have been extensively studied because of their promising properties for chemistry and application in storage of gases,[37,38] separation[39−44], and catalysis.[45−52] Thus, the PCPs with cavities and open channels can be freely accessed by the small molecules, therefore, exhibiting a potential for the use of PCPs or MOFs as the templates for the preparation of nanoporous carbon materials.[53,54]

In the previous works, mesoporous silica with acidic sites has been used as templates for the preparation of mesoporous carbon. The acidic sites walls can accelerate the polymerization of the carbon sources. In order to increase the acidic sites, it is necessary that more amounts of metal species (or metal oxides) are incorporated into the silica walls. However, with an increase in the metal species, well-ordered mesostructures are sometimes distorted or collapsed. To overcome such issues, it is necessary to find an alternative template material with more acidic sites in a stable framework.

In this paper, we focused on Al-PCP [Al(OH)(1,4-NDC)•$2H_2O$], which has Al sites with the organic ligands (1,4-naphthalene dicarboxylic acid). Octahedral $Al(OH)_2O_4$ with 1,4-naphthalenedicarboxylate (1,4-NDC) chains forms the network with two microchannels with square-shaped cross sections, where the large channels represents the size of 7 Å × 7 Å, and the small channels are about 3 Å × 3 Å. The used Al-PCPs accommodate many hydroxyl groups bridging two Al ions, which can act as Brønsted acids[55] to accelerate the polymerization of the carbon sources.[56] Here, we report the preparation of microporous carbon materials by using Al-PCPs and furfuryl alcohol (FA) as the carbon source. We carefully investigated the effect of the loading amount of FA into the porous networks of Al-PCPs on properties of the obtained microporous carbon. The present finding illustrates a new trend of application as a matrix for the preparation of nanoporous carbon and other porous materials. The present work is widely applicable for the preparation of in situ loading of other functional metal−metal oxides within the porous carbon matrix, which is very important as a future application.

2. EXPERIMENTAL SECTION

2.1. Preparation of Microporous Carbon Using Al-PCP. Al-PCP was synthesized according to the previous literature.[57] The light yellow-colored Al-PCP was pretreated under reduced pressure condition (0.01 MPa) at 130 °C for 24 h for the evacuation of water molecules. The degassed Al-PCP (0.25 g) was then mixed with 1.6 g (0.0163 mol) of furfuryl alcohol (FA) and heated at 40 °C in a vacuum oven (0.1 MPa) for 24 h. Polymerization of FA inside the Al-PCP was carried by heating the Al-PCP/FA composite at 80 °C for 24 h and 150 °C for 8 h under nitrogen gas atmosphere. The many hydroxyl groups bridging two Al ions in the Al-PCP can act as Brønsted acids[55] to accelerate the polymerization of the FA.[56] After the polymerization, the above impregnation followed by the polymerization process was repeated one more time. The obtained composites were designated as "Al-PCP-FA_1 composite" and "Al-PCP-FA_2 composite", where the numbers 1 and 2 indicate the number of impregnation times of FA. The amounts of the obtained composites were 0.28 g (for Al-PCP-FA_1 composite) and 0.30 g (for Al-PCP-FA_2 composite), respectively. Therefore, it was roughly calculated that each composite included around 11 wt % (for Al-PCP-FA_1 composite) and 17 wt % polymerized-FA (for Al-PCP-FA_2 composite), respectively.

The carbonization of the Al-PCP-FA composite was performed at 1000 °C for 5 h and then cooled to room temperature, which results in the black powders. Finally, the as-synthesized samples were treated with 10% HF solution in order to remove the alumina particles. The complete removal of the alumina particles was confirmed by energy dispersive X-ray spectroscope (EDX) attached to a TEM machine (Figure S1 of the Supporting Information). The obtained samples were designated as "Al-PCP-FA_1" and "Al-PCP-FA_2", where the numbers 1 and 2 indicates the number of impregnation times of FA. To compare the effect of the impregnation of FA on the formation of microporous carbon, the Al-PCP itself (without the addition of FA) was carbonized at 1000 °C, which is denoted as "Al-PCP-FA_0".

2.2. Characterization. Powder X-ray diffraction measurements (XRD) were performed on an X-ray diffractometer (Rigaku RINT Ultima III) by using Cu Kα radiation (λ = 0.154 nm). The nitrogen adsorption−desorption measurements were carried out at liquid nitrogen temperature (−196 °C) on a Quantachrome Autosorb-1. BET surface area was estimated over a relative pressure range of 0.05−0.3, during which the BET plot is linear. The pore sizes were calculated by using the NLDFT (nonlocalized density functional theory) method. The morphologies of the Al-PCP and Al-PCP-FA composite and the resultant Al-PCP-FA were measured by the SEM images using a HITACHI S-4800 SEM. For transmission election microscopy (TEM), very small amounts of the powder samples were finely dispersed in ethanol with sonication. TEM images were acquired with the JEOL JEM-2000 instrument operated at 200 kV. Raman spectra were recorded at ambient temperature on a photon design spectrometer with an argon ion laser with an excitation wavelength of 520 nm. To understand the carbonization process, three samples (original Al-PCP, Al-PCP-FA_1 composite, and Al-PCP-FA_2 composite) were measured by thermogravimetric (TG) analysis using Seiko TG-DTA 6200. For each sample, a 5.00 mg amount was put on the TG sample holder and measured under inert atmosphere with the heating ramp of 10 °C min^{-1}.

3. RESULTS AND DISCUSSION

Figure 1 shows the SEM images of the original Al-PCP and the obtained microporous carbon materials. From the images, it is very clear that the original Al-PCP morphology was retained even after the conversion to carbon (Figure 1e−h). In our study, the impregnation of FA into the Al-PCP was performed under reduced pressure. The SEM image of the Al-PCP-FA_1 composite before carbonization (Figure 1d) represents the original morphology of Al-PCP. Therefore, the method under the reduced pressure condition effectively avoided the adsorption of guest molecules on the outer surface of the templates. After the carbonization, the wide-angle XRD pattern of Al-PCP-FA_2 after HF treatment (i.e., after removal of alumina) displayed two broad peaks 2θ = 25° and 44° corresponding to the typical peaks of carbon (Figure 2c). For the wide-angle XRD pattern of Al-PCP-FA_2 before HF treatment (i.e., before removal of alumina), several obvious diffractions assignable to γ-alumina (Al_2O_3) crystals were also observed apart from the diffractions corresponding to carbon (Figure 2b). However, after the HF treatment, the γ-alumina phase was completely removed (Figure 2c). In the previous study on preparation of microporous carbon using Zn-based MOF-5, such a chemical treatment was not necessary to remove metal−metal oxide particles, which were formed during the carbonization process.[53,54] This is because ZnO was reduced during the carbonization process at temperatures higher than 800 °C, and then the Zn metal easily vaporized away at

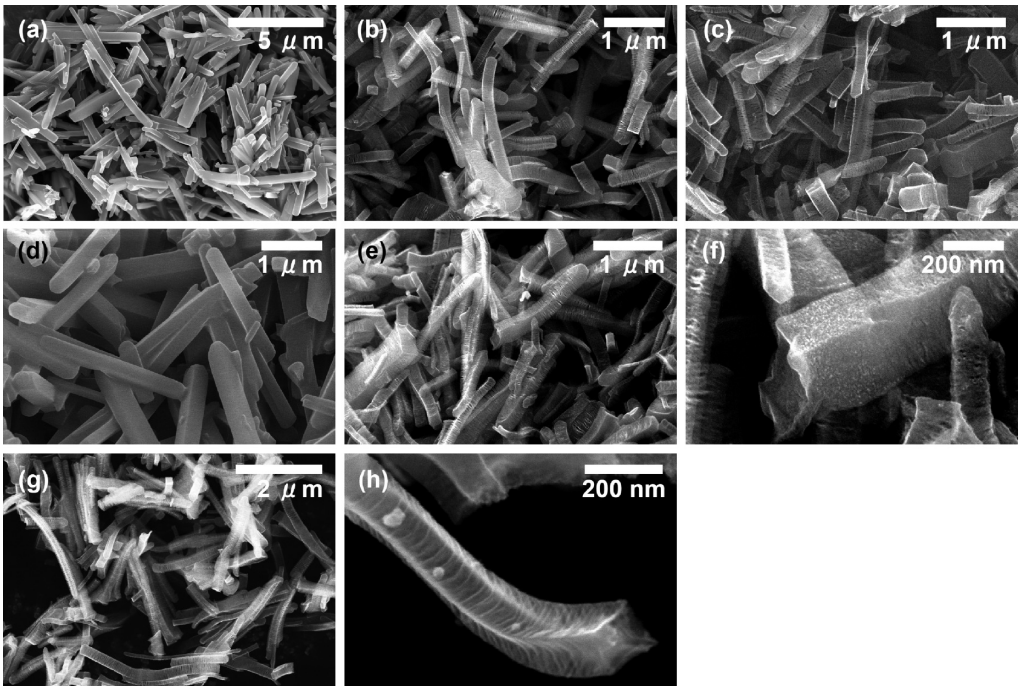

Figure 1. SEM images of (a) original Al-PCP and (b) Al-PCP-FA_0 before removal of alumina, (c) Al-PCP-FA_0 after removal of alumina, (d) Al-PCP-FA_2 composite before carbonization, (e−f) Al-PCP-FA_2 before removal of alumina, and (g−h) Al-PCP-FA_2 after removal of alumina. The very small bright particles observed over the entire area in (f) indicate they formed γ-alumina nanoparticles.

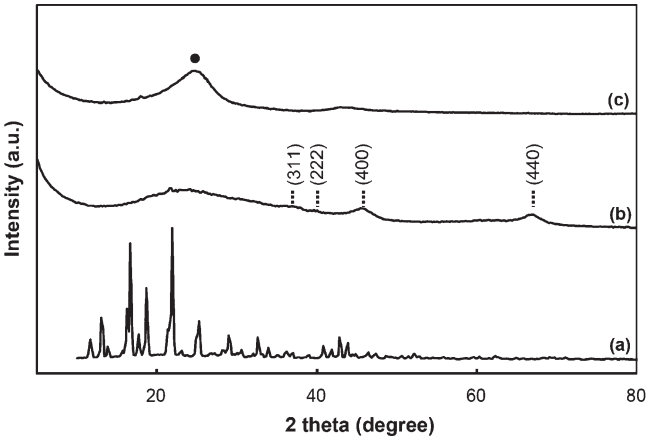

Figure 2. Wide-angle XRD patterns of (a) original Al-PCP and (b) Al-PCP-FA_2 before removal of alumina, and (c) Al-PCP-FA_2 after removal of alumina. In panel (b), several peaks are assignable to (311), (222), (400), and (440) diffractions of γ-alumina crystal. In panel (c), the broad peak assignable to the typical carbon is observed, as indicated by the dot.

around 900 °C. The boiling point of Zn is 908 °C, close to the applied carbonization temperature (1000 °C). However, the melting and boiling points (i.e., vaporization temperature) of Al_2O_3 are extremely higher (2327 °C) rather than the applied carbonization temperature (1000 °C). Therefore, the γ-Al_2O_3 phase cannot be spontaneously removed during the carbonization step itself, and it needs to be removed by chemical treatment only.

Microporous carbon (Al-PCP-FA_2) before and after the removal of γ-Al_2O_3 was investigated by TEM observation (Figures 3 and 4). Before the chemical treatment by HF, alumina nanoparticles were distributed over the entire area of Al-PCP-FA_2, which was more clearly confirmed by the dark field TEM image (Figure 3b). From the highly magnified TEM image, the lattice fringes corresponding to γ-Al_2O_3 nanoparticles were observed, as indicated by the arrows in Figure 3c. The size of the alumina nanoparticles ranged from 2 to 10 nm. In the selected area electron diffraction (ED) patterns, the diffraction rings (400 and 440 diffraction patterns) assignable to the γ-Al_2O_3 phase was overlapped along with the diffraction rings of carbon (Figure 3a, inset). A few sheet-like nanostructures were stacked on each other and were bending in a random order (Figure 3c). After the chemical treatment using HF solution, γ-Al_2O_3 nanoparticles were completely removed, and the respective selected area ED patterns showed no diffraction rings corresponding to the γ-Al_2O_3 (Figure 4). The complete removal of the alumina particles was also confirmed by energy dispersive X-ray spectroscope (EDX) attached with TEM machine (Figure S1 of the Supporting Information).

Nitrogen adsorption−desorption isotherms of Al-PCP-FA_2 before and after the removal of γ-Al_2O_3 are shown in Figure 5. For comparison, Al-PCP-FA_0 and Al-PCP-FA_1 after removal of γ-Al_2O_3 are also shown. The surface areas and total pore volumes are listed in Table 1. The surface areas of the obtained microporous carbon increased significantly with an increase in the number of impregnation steps of FA into the PCPs. The shape of the isotherms of the Al-PCP-FA_2 indicated the existence of both micropores and mesopores (Figure 5). The steep increase at low relative pressure indicates the presence of the micropores. The mesopore sizes were also calculated by using the NLDFT (nonlocalized density functional theory) method. Although Al-PCP-FA_0 and Al-PCP-FA_1 showed no mesoporosity, the Al-PCP-FA_2 possessed the presence of mesopores clearly (Figure S2 of the Supporting Information). The size distribution was observed in the range of the mesopore size, and its peak-top was located at around 5 nm (Figure S2 of the Supporting Information).

dx.doi.org/10.1021/cm102921y |*Chem. Mater.* 2011, 23, 1225–1231

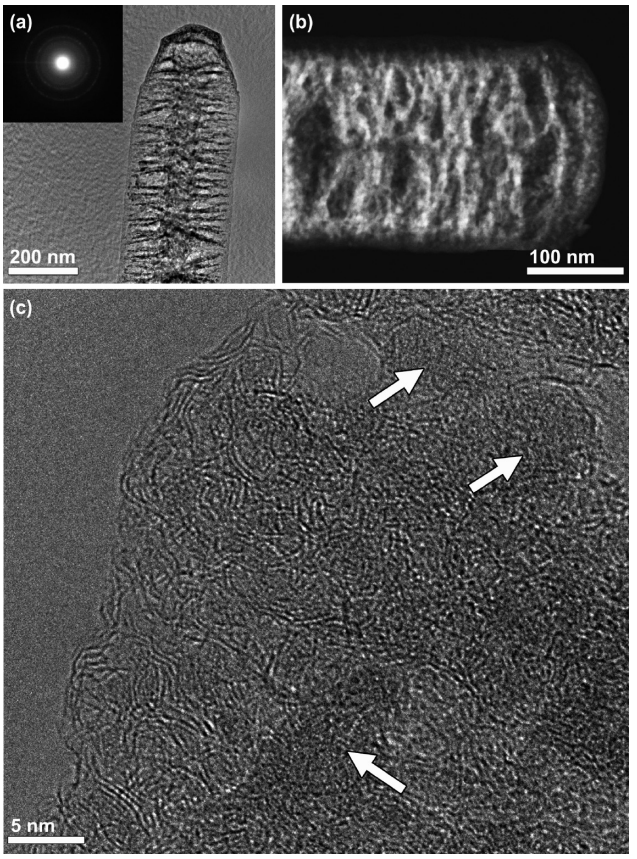

Figure 3. TEM images of Al-PCP-FA_2 before removal of alumina. Panels (a) and (b) are the bright field and dark field images, respectively. Panel (c) is the high resolution bright field image of Al-PCP-FA_2 before removal alumina, and the presence of alumina particles are indicated by the arrow. The inset image in panel (a) is the selected area electron diffraction (SAED) patterns. The inner and outer circular patterns are assigned to the 400 and 440 planes derived from alumina, which overlaps with the diffraction patterns of porous carbon.

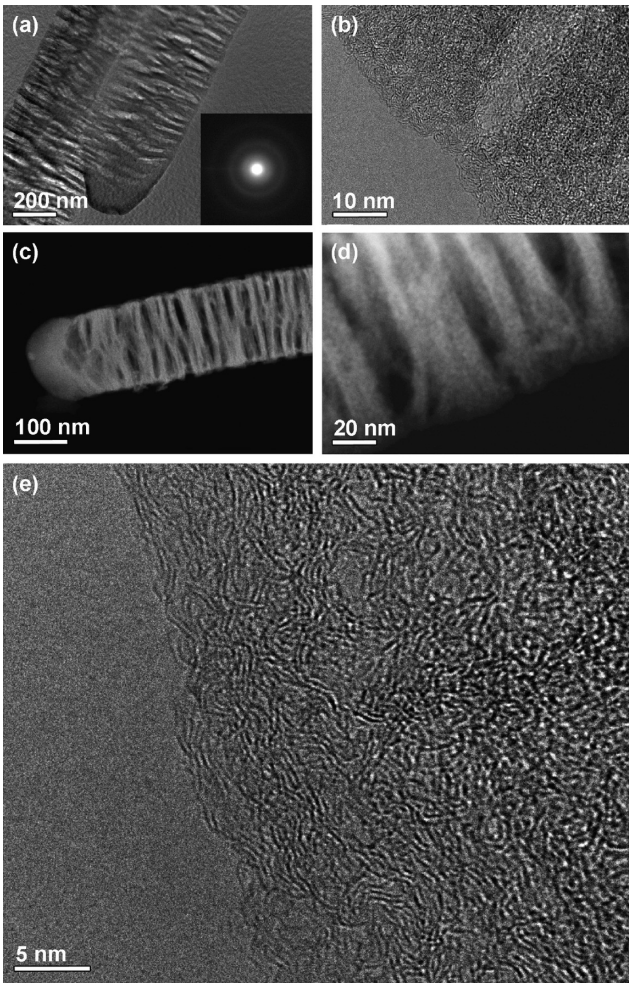

Figure 4. TEM images of Al-PCP-FA_2 after removal of alumina. Panels (a) and (b and e) are low and high magnification bright field images, respectively. Panels (c) and (d) are low and high magnification dark field images, respectively.

From TEM images (Figures 3c and 4e), it was partially observed that the voids with 5 nm in size were formed by a few carbon layers, although their arrangements were disordered and could not be observed clearly in the TEM images. It should be noted that after the removal of γ-Al_2O_3, the pore size distribution of the Al-PCP-FA_2 further broadened, and the mesopores larger than 5 nm were formed (Figure S2c of the Supporting Information). The origin of such mesopores is the voids formed by dissolution of the γ-Al_2O_3 nanoparticles distributed inside the carbon matrix (Figure 3c).

Thermogravimetric (TG) analysis of Al-PCP-FA_1 and Al-PCP-FA_2 composites (before carbonization) was carried out to understand the formation process of the microporous carbons (Figure 6). For comparison, Al-PCP without carbon source (FA) was directly measured. In all cases, two main weight losses were observed. The first step weight loss started at 250 °C and terminated at 450 °C. The corresponding weight loss should be attributed to the loss of unpolymerized FA and solvent molecules accommodated in the cavities of Al-PCP. With the addition of FA to the Al-PCP, the weight loss was increased gradually. The second step of the weight loss between 500 and 600 °C corresponded to the decomposition of the host frameworks. After the decomposition of the organic frameworks, the dispersed Al species were aggregated to form Al_2O_3 matrix. Probably, the crystallization to γ-Al_2O_3 occurred over 900 °C. Thus, in the TG measurement, both the Al-PCP as host frameworks and the polymerized FA as the carbon source showed weight loss. As shown in Figure 6, three samples showed similar weight loss at the end. It was indicated that the total weight loss of the polymerized FA (until conversion to carbon is complete) was almost the same as that of Al-PCP. Actually, it was previously reported that when only polymerized FA was measured by TG analysis (from 100 to 900 °C) about a 50 wt % weight loss was confirmed.[58] Also, the original Al-PCP showed about a 55 wt % weight loss in total (Figure 6). Therefore, we could not confirm large difference of total weight losses at the end among the three samples.

In general, the pore size of the carbon materials replicated by mesoporous silicas (e.g., SBA-15, MCM-48) coincides with the wall thicknesses of the starting mesoporous silicas. However, in our case, the template Al-PCP network represents two square-shaped channels with the size of 0.7 nm × 0.7 nm and 0.3 nm × 0.3 nm, which justified the micropores in the Al-PCP-FA_n (n = 0, 1, and 2). The present work using Al-PCP is quite different from the previous nanocasting process using hard templates. From TG data (Figure 6), the large weight losses were confirmed during the pyrolysis of the polymerized FA in the pores of Al-PCP. It is

Table 1. Surface Areas and Pore Volumes Calculated by N_2 Adsorption−Desorption Isotherms

sample names	surface area (m^2/g)	pore volume (cc/g)
Al-PCP-FA_0	178	0.245
Al-PCP-FA_1	263	0.439
Al-PCP-FA_2	513	0.844
Al-PCP-FA_2 (before alumina removal)	343	0.402

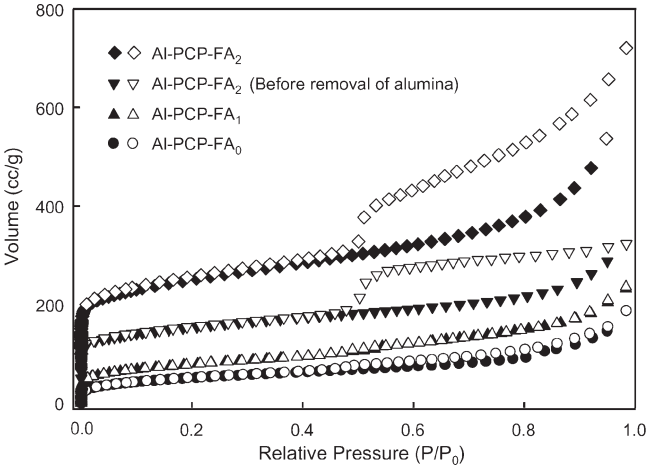

Figure 5. Nitrogen adsorption−desorption isotherms of (●○) Al-PCP-FA_0 after removal of alumina, (▲Δ) Al-PCP-FA_1 after removal of alumina, (▼▽) Al-PCP-FA_2 before removal of alumina, and (■□) Al-PCP-FA_2 after removal of alumina. Adsorption and desorption isotherms are indicated by the filled and open symbols, respectively.

indicated that the pore space in the Al-PCP was not completely filled by the FA sources.

Furthermore, during the carbonization process, the Al-PCP framework itself thermally shrinks. Thus, unlike mesoporous silicas, the Al-PCP cannot act as a direct template. Insufficient loading of the FA collapsed the original nanospace of the Al-PCP by the thermal shrinkage (Table 1). With an increase in the FA amount by the impregnation steps, the nanospace originated from the Al-PCP effectively can remain after the carbonization process (Table 1).

Raman spectroscopy was carried out to obtain further information on the surface and topology of porous carbon materials. In Figure 7, the spectra exhibits D and G bands at 1355 cm^{-1} and 1585 cm^{-1}, respectively, corresponding to the defects/disordered structures in the carbon and vibrational mode to the movement in opposite directions of two carbon atoms in a single crystal graphite sheet. The relative intensity (I_D/I_G) ratios were almost constant with an increase in the loading FA amount. In general, the relative intensity ratio is proportional to the number of defects in graphitic carbon. The degree of graphitization in the obtained microporous carbons (Al-PCP-FA_0 Al-PCP-FA_1, and Al-PCP-FA_2) was not changed very much.

It is important to note that in our process we could successfully replicate the fibrous morphology of the original Al-PCP (Figure 1) by using FA as the carbon source. Liu et al. prepared microporous carbon material using MOF-5 as a template.[53,54] They used FA as the carbon source and introduced the vapor of the FA into the pores of the MOF-5. However, they could not

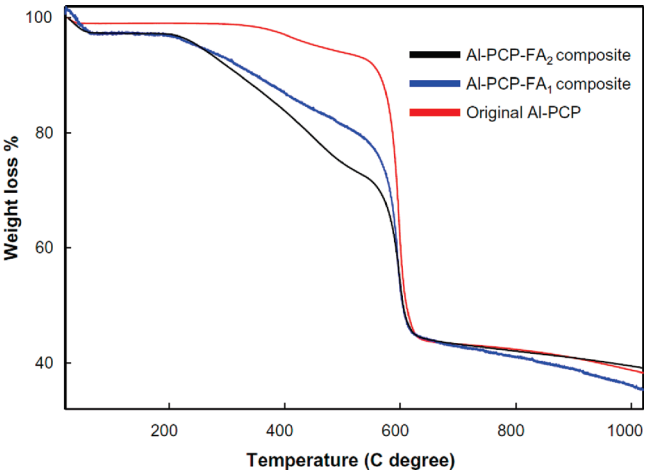

Figure 6. TG curves of original Al-PCP, Al-PCP-FA_1 composite, and Al-PCP-FA_2 composite before carbonization.

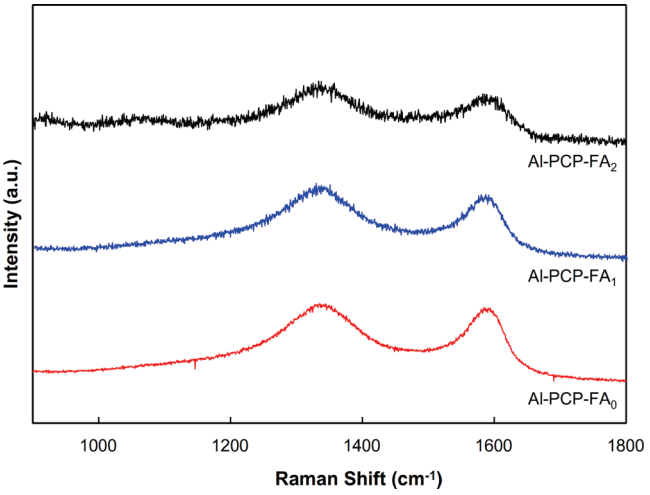

Figure 7. Raman spectra of Al-PCP-FA_0, Al-PCP-FA_1, and Al-PCP-FA_2 after the removal of alumina.

show the replication of the morphology of the original template. To realize the perfect replication of the morphology, the molecular dimension and the size of the used carbon source should be considered. Carbon sources with larger molecular dimensions become impossible for the loading/impregnation into the pores of the template materials. In the general preparation of carbon replicas using mesoporous silicas, polymerized sucrose has been used as the carbon source (i.e., sucrose molecules are polymerized before the impregnation step.).[10−14] It is easy for polymerized sucrose to load into the mesoporous silicas with larger pore size.[10−14] When we used polymerized sucrose as the carbon source, the morphological replication was not successful (Al-PCP-Suc). From the SEM images (Figure S3 of the Supporting Information), the unsuccessful replication of morphology of the parent Al-PCP was clearly confirmed. The reason for the failure is that the size of the polymerized sucrose molecule is larger than the square-shaped channels of the used Al-PCP. The polymerized sucrose molecule, which has larger molecular dimensions, finds it difficult to impregnate inside the pores of the Al-PCP.

On the other hand, unpolymerized FA used in this study has molecular dimension of 8.4 Å × 6.4 Å × 4.2 Å, which is smaller

dx.doi.org/10.1021/cm102921y |*Chem. Mater.* 2011, 23, 1225–1231

than the Al-PCP pore channels, and it can be widely used as the carbon source, especially for the preparation of microporous carbon materials. The FA is particularly attractive because FA is liquid at room temperature and readily miscible with water and many organic solvents. Moreover, it can be polymerized at various conditions such as vapor and liquid under heating at various temperatures and/or in the presence of a flexible choice of catalysts. Hence, we consider that FA is more suitable as the carbon source in our present work than other carbon sources.

Apart from the size of the carbon source, the influence and interaction of the template on the polymerization of the carbon source must be considered. There have been several reports on polymerization of FA monomer molecules into poly(furfuryl alcohol) by utilizing acids and/or catalysts.[59−63] The polymerization step is a process of reacting monomer molecules together in a chemical reaction to form three-dimentional networks or polymer chains. As explained already, the Al-PCP accommodates many hydroxyl groups bridging two Al ions, which can act as Brønsted acids[55] for the polymerization of FA guest monomer molecules.[56] Therefore, during the impregnation process, the furfuryl alcohol molecules penetrate into the Al-PCP pore channels and react with acidic sites of the template. The resulting rigid Al-PCP composite with polymerized FA easily transforms into carbonaceous chains at high temperature.

4. CONCLUSION

We successfully prepared microporous carbon fibers through carbonization of an Al-based porous coordination polymer (Al-PCP) with furfuryl alcohol (FA) as the carbon source. From SEM and TEM observation, the original fibrous morphology of Al-PCP was successfully replicated in the products. During the carbonization process, Al species were aggregated to form γ-alumina nanoparticles. The size of the alumina nanoparticles ranged from 2 to 10 nm, and they were well distributed over the entire area. By chemical treatment with HF, the alumina was easily removed to obtain pure carbon with a microporous structure. With an increase in the amount of FA loading into the Al-PCP, both the surface areas and pore volumes of the microporous carbons were gradually increased up to 513 m^2/g and 0.844 cc/g, respectively. The present finding illustrates a new trend of application as a matrix for the preparation of nanoporous carbon and other porous materials. In another viewpoint, the present work can be applicable for the preparation of in situ loading of functional metal−metal oxides (such as alumina, iron oxide) within the porous carbon matrix, which is very important as a future application. These types of functional nanoporous carbons can be applied as magnetically separable materials and highly active catalysts.

■ ASSOCIATED CONTENT

Supporting Information. Figure S1: EDX spectra of Al-PCP-FA_2 before removal of alumina and Al-PCP-FA_2 after removal of alumina. Figure S2: Pore size distribution calculated by NLDFT method. Figure S3: Low and high magnification of Al-PCP-Suc. This material is available free of charge via the Internet at http://pubs.acs.org.

■ AUTHOR INFORMATION

Corresponding Author
*Yamauchi.Yusuke@nims.go.jp.

■ REFERENCES

(1) Liang, C.; Li, Z.; Dai, S. *Angew. Chem., Int. Ed.* **2008**, *47*, 3696.
(2) Lee, J.; Kim, J.; Hyeon, T. *Adv. Mater.* **2006**, *18*, 2073.
(3) Zheng, B.; Lu, C.; Gu, G.; Makarovski, A.; Finkelstein, G.; Liu, J. *Nano Lett.* **2002**, *2*, 895.
(4) Thess, A.; Lee, R.; Nikolaev, P.; Dai, H.; Petit, P.; Robert, J.; Xu, C.; Lee, Y. H.; Kim, S. G.; Rinzler, A. G.; Colbert, D. T.; Scuseria, G. E.; Tománek, D.; Fischer, J. E.; Smalley, R. E. *Science* **1996**, *273*, 483.
(5) Journet, C.; Maser, W. K.; Bernier, P.; Loiseau, A.; Lame de la Chapelle, M.; Lefrant, S.; Deniard, P.; Lee, R.; Fischer, J. E. *Nature* **1997**, *388*, 756.
(6) Lu, A. H.; Schüth, F. *Adv. Mater.* **2006**, *18*, 1793.
(7) Lu, A. H.; Schüth, F. *C. R. Chim.* **2005**, *8*, 609.
(8) Ryoo, R.; Joo, S. H.; Jun, S. *J. Phys. Chem. B* **1999**, *103*, 7743.
(9) Kaneda, M.; Tsubakiyama, T.; Carlsson, A.; Sakamoto, Y.; Ohsuna, T.; Terasaki, O.; Joo, S. H.; Ryoo, R. *J. Phys. Chem. B* **2002**, *106*, 1256.
(10) Lu, A.-H.; Schmidt, W.; Taguchi, A.; Spliethoff, B.; Tesche, B.; Schüth, F. *Angew. Chem., Int. Ed.* **2002**, *41*, 3489.
(11) Kang, M.; Yi, S. H.; Lee, H. I.; Yie, J. E.; Kim, J. M. *Chem. Commun.* **2002**, 1944.
(12) Jun, S.; Joo, S. H.; Ryoo, R.; Kruk, M; Jaroniec, M.; Liu, Z.; Ohsuna, T.; Terasaki, O. *J. Am. Chem. Soc.* **2000**, *122*, 10712.
(13) Shin, H. J.; Ryoo, R.; Kruk, M.; Jaroniec, M. *Chem. Commun.* **2001**, 349.
(14) Lee, J.-S.; Joo, S. H.; Ryoo, R. *J. Am. Chem. Soc.* **2002**, *124*, 1156.
(15) Ryoo, R.; Joo, S. H.; Jun, S.; Tsubakiyama, T.; Terasaki, O. *Stud. Surf. Sci. Catal.* **2001**, *135*, 150.
(16) Kim, T.-W.; Ryoo, R.; Gierszal, K. P.; Jaroniec, M.; Solovyov, L. A.; Sakamoto, Y.; Terasaki, O. *J. Mater. Chem.* **2005**, *15*, 1560.
(17) Kyotani, T.; Nagai, T.; Inoue, S.; Tomita, A. *Chem. Mater.* **1997**, *9*, 609.
(18) Rodriguez-Mirasol, J.; Cordero, T.; Radovic, L. R.; Rodriguez, J. J. *Chem. Mater.* **1998**, *10*, 550.
(19) Ma, Z.; Kyotani, T.; Tomita, A. *Chem. Commun.* **2000**, 2365.
(20) Ma, Z.; Kyotani, T.; Liu, Z.; Terasaki, O.; Tomita, A. *Chem. Mater.* **2001**, *13*, 4413.
(21) Johnson, S. A.; Brigham, E. S.; Ollivier, P. J.; Mallouk, T. E. *Chem. Mater.* **1997**, *9*, 2448.
(22) Mulfort, K. L.; Hupp, J. T. *J. Am. Chem. Soc.* **2007**, *129*, 9604.
(23) Pan, L.; Olson, D. H.; Ciemnolonski, L. R.; Heddy, R.; Li, J. *Angew. Chem., Int. Ed.* **2006**, *45*, 616.
(24) Panella, B.; Hirscher, M. *Adv. Mater.* **2005**, *17*, 538.
(25) Eddaoudi, M.; Kim, J.; Rosi, N.; Vodak, D.; Wachter, J.; O'Keeffe, M.; Yaghi, O. M. *Science* **2002**, *295*, 469.
(26) Chen, B.; Eddaoudi, M.; Hyde, S. T.; O'Keeffe, M.; Yaghi, O. M. *Science* **2001**, *291*, 1021.
(27) Li, H.; Eddaoudi, M.; O'Keeffe, M.; Yaghi, O. M. *Nature* **1999**, *402*, 276.
(28) Yaghi, O. M.; O'Keeffe, M.; Ockwig, N. W.; Chae, H. K.; Eddaoudi, M.; Kim, J. *Nature* **2003**, *423*, 705.
(29) Kitagawa, S.; Kitaura, R.; Noro, S. *Angew. Chem., Int. Ed.* **2004**, *43*, 2334.
(30) Férey, G.; Mellot-Draznieks, C.; Serre, C.; Millange, F. *Acc. Chem. Res.* **2005**, *38*, 217.
(31) Bradshaw, D.; Claridge, J. B.; Cussen, E. J.; Prior, T. J.; Rosseinsky, M. J. *Acc. Chem. Res.* **2005**, *38*, 273.
(32) Morris, R. E.; Wheatley, P. S. *Angew. Chem., Int. Ed.* **2008**, *47*, 4966.
(33) Dincá, M.; Long, J. R. *Angew. Chem., Int. Ed.* **2008**, *47*, 6766.
(34) Wang, Z.; Cohen, S. M. *Chem. Soc. Rev.* **2009**, *38*, 1315.
(35) Mueller, U.; Schubert, M.; Teich, F.; Puetter, H.; Schierle-Arndt, K.; Pastre, J. *J. Mater. Chem.* **2006**, *16*, 626.
(36) Zacher, D.; Shekhah, O.; Woll, C.; Fischer, R. A. *Chem. Soc. Rev.* **2009**, *38*, 1418.
(37) Férey, G.; Latroche, M.; Serre, C.; Milange, F.; Loiseau, T.; Percheron-Guégan, A. *Chem. Commun.* **2003**, 2976.

(38) Rosi, N. L.; Eckert, J.; Eddaoudi, M.; Vodak, D. T.; Kim, J.; O'Keeffe, M.; Yaghi, O. M. *Science* **2003**, *300*, 1127.
(39) Cychosz, K. A.; Wong-Foy, A. G.; Matzger, A. J. *J. Am. Chem. Soc.* **2008**, *130*, 6938.
(40) Finsy, V.; Verelst, H.; Alaerts, L.; Vos, D. D.; Jacobs, P. A.; Baron, G. V.; Denayer, J. F. M. *J. Am. Chem. Soc.* **2008**, *130*, 7110.
(41) Bradshaw, D.; Prior, T. J.; Cussen, E. J.; Claridge, J. B; Rosseinsky, M. J. *J. Am. Chem. Soc.* **2004**, *126*, 6106.
(42) Dybtsev, D. N.; Chun, H.; Yoon, S. H.; Kim, D.; Kim, K. *J. Am. Chem. Soc.* **2004**, *126*, 32.
(43) Min, K. S.; Suh, M. P. *Chem.—Eur. J.* **2001**, *7*, 303.
(44) Wang, B.; Côté, A. P.; Furukawa, H.; O'Keeffe, M.; Yaghi, O. M. *Nature* **2008**, *453*, 207.
(45) Fujita, M.; Know, Y. J.; Washizu, S.; Ogura, K. *J. Am. Chem. Soc.* **1994**, *116*, 1151.
(46) Lee, J.; Farha, O. K.; Roberts, J.; Scheidt, K. A.; Nguyen, S. T.; Hupp, J. T. *Chem. Soc. Rev.* **2009**, *38*, 1450.
(47) Ma, L.; Abney, C.; Lin, W. *Chem. Soc. Rev.* **2009**, *38*, 1248.
(48) Hasegawa, S.; Horike, S.; Matsuda, R.; Furukawa, S.; Mochizuki, K.; Kinoshita, Y.; Kitagawa, S. *J. Am. Chem. Soc.* **2007**, *129*, 2607.
(49) Horike, S.; Dinc, M.; Tamaki, K.; Long, J. R. *J. Am. Chem. Soc.* **2008**, *130*, 5854.
(50) Cho, S. H.; Ma, B.; Nguyen, S. T.; Hupp, J. T.; Albrecht-Schmitt, T. E. *Chem. Commun.* **2006**, 2563.
(51) Ingleson, M. J.; Barrio, J. P.; Bacsa, J.; Dickinson, C.; Park, H.; Rosseinsky, M. J. *Chem. Commun.* **2008**, 1287.
(52) Gallopin, T.; Fort, P.; Eggermann, E.; Cauli, B.; Luppi, P.-H.; Rossier, J.; Audinat, E.; Mühlethaler, M.; Serafin, M. *Nature* **2000**, *404*, 982.
(53) Liu, B.; Shioyama, H.; Akita, T.; Xu, Q. *J. Am. Chem. Soc.* **2008**, *130*, 5390.
(54) Liu, B.; Shioyama, H.; Jiang, H.; Zhang, X.; Xu, Q. *Carbon* **2010**, *48*, 456.
(55) Ravon, U.; Chaplais, G.; Chizallet, C.; Seyyedi, B.; Bonino, F.; Bordiga, S.; Bats, N.; Farrusseng, D. *ChemCatChem* **2010**, *2*, 1235.
(56) Bertarione, S.; Bonino, F.; Cesano, F.; Damin, A.; Scarano, D.; Zecchina, A. *J. Phys. Chem. B* **2008**, *112*, 2580.
(57) Comotti, A.; Bracco, S.; Sozzani, P.; Horike, S.; Matsuda, R.; Chen, J.; Takata, M.; Kubota, Y.; Kitagawa, S. *J. Am. Chem. Soc.* **2008**, *130*, 13664.
(58) Manocha, S. M.; Vashistha, D. Y.; Manocha, L. M. *J. Mater. Sci. Lett.* **1997**, *16*, 705.
(59) Pranger., L.; Tannenbaum, R. *Macromolecules* **2008**, *41*, 8682.
(60) Principe, M.; Martínez, R.; Ortíz, P.; Rieumont, J. *Polimeros Ciencia e Technologia* **2000**, *10*, 8.
(61) Gandhini, A. *Adv. Polym. Sci.* **1977**, *25*, 47.
(62) González, R.; Martínez, R.; Ortíz, P. *Makromol Chem. Rapid Commun. (Macromol. Rapid Commun.* **1992**, *13*, 517.
(63) Krishnan, T. A.; Chanda, M. *Die Angew. Makromol. Chem. (Macromol. Mater. Eng)* **1975**, *43*, 145.